

3D Non-Linear Modeling and Its Effects in Earthquake Soil-Structure Interaction

Sumeet Kumar Sinha¹, Yuan Feng¹, Han Yang¹, Hexiang Wang¹, Nebojša Orbović²
David B. McCallen³, Boris Jeremić^{1,3}

¹ Department of Civil and Environmental Engineering, UC Davis, CA, USA

² Canadian Nuclear Safety Commission, Ottawa, ON, Canada

³ Earth and Environmental Science Area, LBNL, Berkeley, CA, USA

ABSTRACT

Modeling and simulation of earthquake soil-structure interaction (ESSI) requires number of sophisticated modeling and simulation approaches in order to reduce modeling uncertainty and to improve the accuracy of results. Of particular importance here, is the non-linear effects, that control the Earthquake Soil-Structure Interaction (ESSI) behavior for any significant seismic event. Non-linear response of soil and rock, of the contact zone (soil/rock-foundation), base isolators and dissipators, and of the structural components prove sometimes beneficial and sometimes detrimental to the overall ESSI response. Present here, is a high fidelity realistic 3D ESSI modeling and simulation approach for a prototype of nuclear power plant (NPP) building. Number of sophisticated modeling approaches that are used for ESSI analysis is presented. Differences between results obtained using elastic soil and elastic-plastic soil with and without contact is discussed. The study illustrates the need for high fidelity modeling to reduce the modeling uncertainty introduced in results when unwarranted simplifications are made.

INTRODUCTION

Seismic simulations to structures are often done by 1-D input excitations defined from a family of damped response spectra. These input motions are applied uniformly to the entire base of the structure regardless of its dimension and dynamic characteristics of the soil, foundation and motion itself. This not only ignores the foundation and its contact with soil, soil-structure interaction (SSI) but also the 3D nature and variability of seismic waves.

Interest to study SSI effects has grown significantly in recent years. However Tyapin (2007) and Lou et al. (2011) note that even after four decades of extensive SSI research, there still exists a large gap. Lou et al. (2011) notes that spatial analysis of full model in 3D is hardly done. To reduce the amount of calculations, many existing publications simplify extremely the super-structure to spring mass damper model or consider only limited interaction. Elgamal et al Elgamal et al. (2008) performed a 3D analysis of a full soilbridge system, focusing on interaction of liquefied soil in foundation and bridge structure. Jeremić et al. (2009) showed a full 3D soil-structure interaction of a prototype bridge, devised as a part of grand challenge, pre-NEESR project.

Investigations of SSI have shown that the dynamic response of a structure supported on elastic-plastic soil may differ significantly from the response of the same structure when supported on a rigid base Chopra & Gutierrez (1974), Bielak (1978). The difference comes because of the dissipation of part of the vibrational energy (seismic energy) by hysteresis action of the soil or structure itself. This results in damping of high frequency components, which could potentially prove quite useful for equipment that are prone to damage

from high frequencies. On the other hand Jeremić et al. (2004) found that SSI can have detrimental effects on structural behavior as well and is dependent on the dynamic characteristics of the earthquake motion, the foundation soil and the structure.

Dissipation of energy during seismic events is another important factor to consider in design for its safety and economy. Dissipating energy in structure can lead to material degradation and damage. It is desired to dissipate most of the energy in soil with acceptable level of deformations in structure. A common neglect of plastic free energy has been observed in many publications, which results in clear violation of the second law of thermodynamics. A thermomechanical framework that can correctly evaluate energy transformation and dissipation in dynamic SSI simulation was presented by Yang et al. (2017), Yang & Jeremić (2017) based on works of Rosakis et al. (2000), Dafalias et al. (2002). This framework is applied to the prototype NPP model that is being analyzed in this paper. Locations with high possibility of damage are identified and insights on design improvement are discussed.

Only a few full 3D SSI interactions have been studied that too mainly focusing on bridges or small soil-foundation system. However, as per authors knowledge a full 3D non-linear analysis for a structure with soil-foundation-structure and contact effects have not been investigated. Purpose of this paper here is to present a methodology for high fidelity modeling of seismic soilfoundation-structure (SFSI) interaction for a prototype of Nuclear Power Plant (NPP) with surface (shallow) foundation. Presented methodology employs the currently best available models and simulation procedures. In addition to presenting such state-of-the-art modeling, simulation results are used to illustrate non-linear-effects on seismic response of a prototype NPP model.

MODEL DEVELOPMENT AND SIMULATION DETAILS

The Nuclear Power Plant (NPP) modeled here is a symmetric structure with shallow foundation of thickness 3.5m and size 100m. Figure 1a shows a slice view of the model in normal y direction (perpendicular to plane of the paper). Solid brick elements were used to model soil and foundation. The NPP structure was modelled by elastic shell elements. This section describes the material and modeling parameters summarized in Table 2, foundation, structure, and contact. Given also is a brief description of staged loading and seismic force application using domain reduction method (DRM).

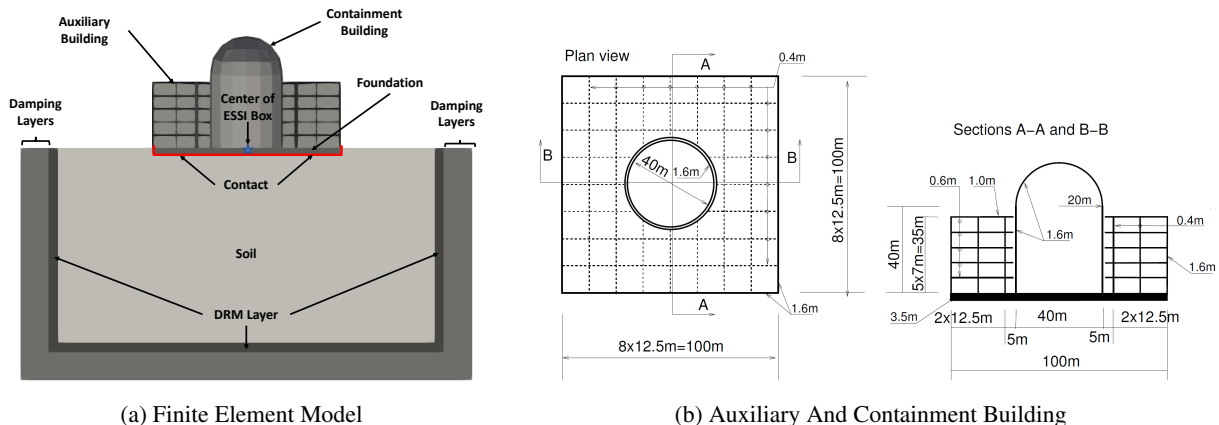


Figure 1: Nuclear power plant model with shallow foundation.

Structure Model

The NPP structure consists of auxiliary building, containment building and shallow foundation as shown in Figure 1b. The auxiliary building consists of 4 floors of 0.6m thickness, ceiling floor of 1m thickness, exterior wall of 1.6m thickness and interior walls of 0.4m thickness. The exterior and interior walls are

Soil	Unit weight, γ [kPa]	21.4	Structure	Unit weight, γ [kPa]	24.0
	Shear velocity, V_s [m/s]	500		Young's modulus, E [GPa]	20
	Young's modulus, E [GPa]	1.3		Poisson's ratio, ν	0.21
	Poisson's ratio, ν	0.25	Contact	Initial normal stiffness, k_n^{init} [N/m]	1e9
	Shear strength, S_u [kPa]	650		Stiffening rate, S_r [/m]	1000
	von Mises radius, k [kPa]	60		Maximum normal stiffness, k_n^{max} [N/m]	1e12
	linear kinematic hardening, h_a [Mpa]	30		Tangential stiffness, k_t [N/m]	1e7
non-linear kinematic hardening, c_r	25	Normal damping, c_n [Ns/m]		100	
Structure	Unit weight, γ [kPa]	24.0	Tangential damping, c_t [Ns/m]	100	
	Young's modulus, E [GPa]	20	Friction ratio, μ	0.25	
	Poisson's ratio, ν	0.21			

Figure 2: Modeling parameters.

embedded down to the depth of the foundation. The containment building is a cylinder of diameter 20m and height 40m with wall thickness of 1.6m. There is a gap of 0.2m between the containment and auxiliary building. Top of the containment building is covered by semi-spherical dome of radius 20m. The foundation is square shallow footing of size 100m and thickness 3.5m. The containment building and the auxiliary building were modelled as shell elements and foundation as linear brick elements, both having the properties of concrete of elastic Youngs modulus 20GPa, poisons ratio 0.21 and density 2400kg/m³. The containment building which is more flexible than the auxiliary building had its first mode as bending with fundamental frequency at 4Hz.

Soil Model

The depth of the soil modelled below the foundation was 120 m, which is also the depth of DRM layer Sec 3.5. It is assumed that within this range the soil will plastify because of its self-weight, structure and seismic motions. The soil is assumed to be a stiff saturated-clay with undrained behavior having shear velocity of 500 m/s, unit weight of 21.4 kPa and Poisson's ratio of 0.25. To represent the travelling wave accurately for a given frequency, about 10 nodes per wavelength i.e. about 10 linear or 3 quadratic brick elements are required. Here, the seismic waves are analyzed up to $f_{max} = 10Hz$. The smallest wavelength λ_{min} to be captured thus, can be estimated as

$$\lambda_{min} = v/f_{max} \quad (1)$$

where, v is the smallest shear wave velocity of interest. For $v = 500m/s$ and $f_{max} = 10Hz$ the minimum wavelength λ_{min} would be $(500m/s)(10/s) = 50m$. Choosing 10 nodes/elements per wavelength the element size would be 5m. Jeremić et al. (2009), Watanabe et al. (2016) state that even by choosing mesh size $\Delta h = \lambda_{min}/10$, smallest wavelength that can be captured with confidence is $\lambda = 2\Delta h$ i.e. a frequency corresponding to $5f_{max}$. Based on the above analysis, soil was modeled as linear 8-node brick elements with grid spacing of $\Delta h = 5m$.

Because of the complex plastic-behavior of the soil many sophisticated models Yang et al. (2003), Dafalias & Manzari (2004) have been developed to capture the non-linear response of soil. Wair et al. (2012) provides an empirical correlation to predict the shear strength of soil for given shear velocity V_s . Dickenson (1994) proposed the following relationship Eq 2 between V_s and undrained strength S_u for cohesive soils in San Francisco Bay Area.

$$V_s[m/s] = 23(S_u[kPa])^{0.475} \quad (2)$$

Thus, for $V_s = 500m/s$, the undrained strength S_u would be 650kPa. Here, two scenarios of soil properties were considered in analysis. One linear elastic and the other as von-Mises with non-linear kinematic hardening of Armstrong Frederick type. For S_u of 650kPa and $E = 1.3Gpa$, the non-linear inelastic model was calibrated for yield strength achieved at 0.01% shear strain with linear kinematic hardening rate (h_a)

as 30MPa and non-linear hardening rate (c_r) as 25. The soil properties is summarized in Table 2. The stress-strain response for the non-linear material model is shown in Figure 3a

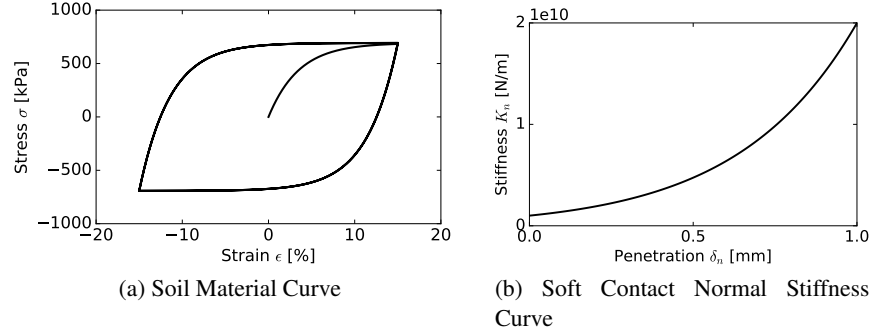


Figure 3: Soil and interface modeling.

Interface Modeling

Node-to-node penalty based soft contact (interface) element Sinha & Jeremić (2017) was used to model the interaction between foundation and soil as they are not one continuum material. In soft contact, normal contact force F_n from soft-soil is assumed to increase exponentially with penetration δ_n as shown in Eq 3. The normal force F_n and stiffness K_n are defined as

$$\begin{aligned} F_n &= k_n^{init} * \exp(S_r * \delta_n) * \delta_n \\ K_n &= \max(k_n^{init} * \exp(S_r * \delta_n) * (1 + k_n^{init} * \delta_n), k_n^{max}) \end{aligned} \quad (3)$$

where δ_n refers to the relative displacement between contact node pairs in normal contact direction, k_n^{init} refers to the normal stiffness in normal contact direction, S_r refers to the stiffening rate in normal contact direction. k_n^{Max} refers to maximum normal stiffness and provides a cap on exponentially increasing stiffness to make the solution numerically stable. The soft contact was implemented to capture the phenomenon of increasing stiffness of soil with increasing penetration. Figure 3b shows the stiffness curve with penetration for the chosen contact parameters also shown in Table 2.

Contact elements were applied all around the foundation connecting to the soil as shown in Figure 1a in red color zone. To ensure the stability of the numerical solution, the penalty stiffness in normal direction was chosen 2 – 3 order magnitude greater than the stiffness of the soil. The Coulombs friction coefficient μ between the soil and the foundation was chosen as 0.25. Viscous damping of 100Ns/m in normal and tangential damping was provided to model viscous damping arising from water.

Seismic Motions

3D seismic motions were developed by Rodgers (2017) using SW4 (Serpentine Wave Propagation of 4th order) Petersson & Sjögreen (2017) for an earthquake of magnitude (M_w) of 5.5 modelled with a point source on a fault of dimension $5.5 \times 5.6km$ with up-dip rupture slip model. The ESSI (Earthquake Soil Structure Interaction) box to capture the free-field motion was located on the foot-wall of the reverse thrust fault. The generated motion had a directivity effect as the fault slips and propagates in x-direction. Also, since the ESSI box was located perpendicular to the fault, strong motions in y-direction were expected.

Acceleration and displacement time-series of the motion at the center of ESSI box is shown in Figure 4. The peak ground acceleration (PGA) in x and y direction is about 0.5g. Significant amount of vertical motions PGA of 0.2g can be observed which is neglected in many conventional seismic simulations. Since, the fault is located at foot-wall side of reverse thrust fault, there is permanent subsidence of about 50mm

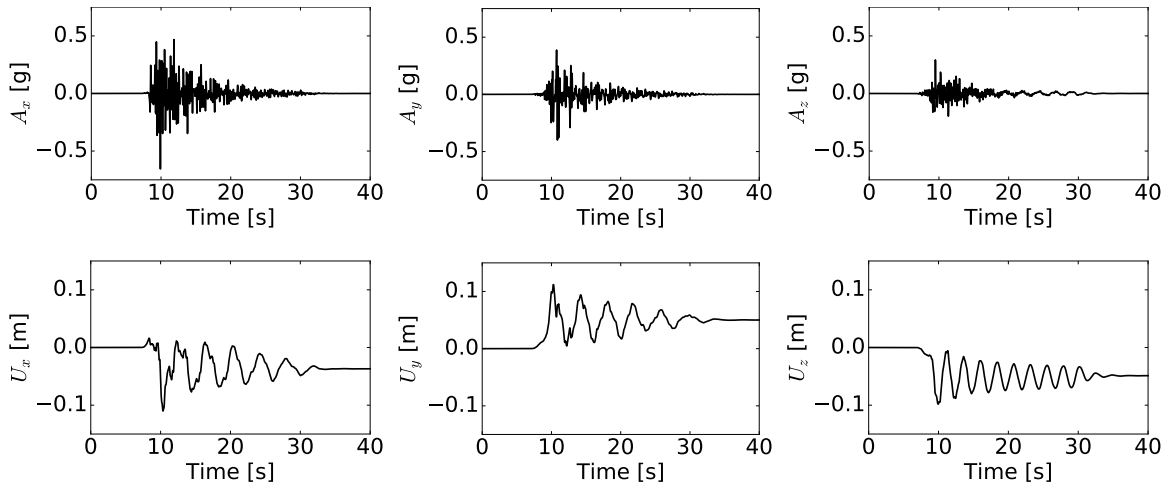


Figure 4: Acceleration and displacement time series.

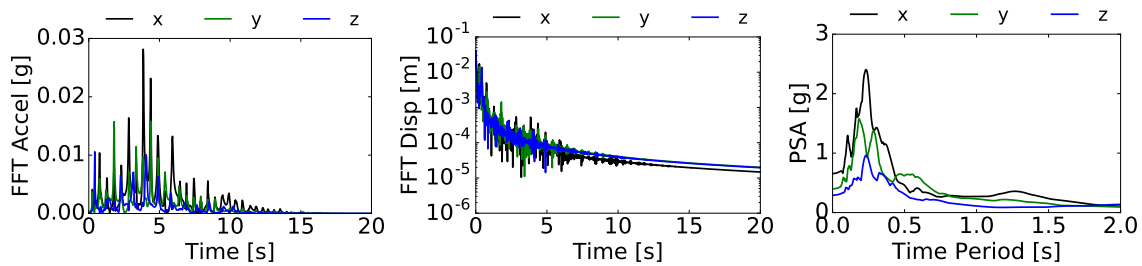


Figure 5: Strong motion Fourier transform and response spectrum.

in z-direction at the end of shaking event. Fourier transform and response spectrum of the motions are shown in Figure 5. The frequency range of the motion is within $20Hz$. Response spectrum plot shows amplification for natural frequency greater than $2Hz$. Since, many equipments in nuclear industry operate at high frequencies, determination of high frequency excitation of NPP building is critical for design.

Domain Reduction Method

Domain Reduction Method (DRM) Bielak et al. (2003) was used to apply 3D seismic motions generated from SW4 all around the model as shown in Figure 1a. DRM is one of the best methods that can apply free field 3D ground motions to a finite-element model. It features a two-stage strategy for a complex, realistic 3D earthquake engineering simulation. First, is the generation of free field model with correct geology and second is the application of the generated free-field to the structure of interest. The DRM layer here is modeled as a single layer of elastic soil. Three damping (absorbing) layers adjacent to DRM layer were modeled to prevent incoming of reflected waves. For this analysis, 60% Rayleigh damping was applied in each of the damping and DRM layers. The Rayleigh damping was applied in the frequency range of 1-5Hz.

Staged Simulation

The whole analysis was simulated with two loading stages. First stage was static self-weight to get the initial stress state of the soil and contact elements. In second stage, seismic motion was applied using DRM method. For each stage, equilibrium was achieved using full Newton-Raphson method with a small tolerance of $1e^{-4}N$ on second-norm of unbalanced force. For dynamic analysis, Newmark integration method with numerical damping $\gamma = 0.7$ was used. Rayleigh damping of 2% in structure and 30% in soil was applied. The time step considered here was 0.02 seconds with simulation running in total for 40 seconds.

The analysis was run in parallel in Real ESSI (Realistic Earthquake-Soil-Structure Interaction) Simulator Jeremić et al. (2017) on eight CPUs. The model consisted of about 300k degrees of freedoms (dofs). Four scenarios (a) elastic no contact (b) elastic with contact (c) elastic-plastic no contact and (d) elastic-plastic with contact were performed. In this paper, unless specified *elastic* means elastic without contact and *inelastic* means elastic-plastic with contact.

SIMULATION RESULTS

Due to the space restriction, only few locations are selected to study the non-linear effects on NPP structure. The selected locations are shown in Figure 6. Since the containment building is more flexible than auxiliary building, location (D) in Figure 6 located on the top of the containment building is naturally the point of interest as it describes maximum drift during shaking. Three locations (A), (B) and (C) located at center of foundation is also selected to study the slip at interface during shaking.

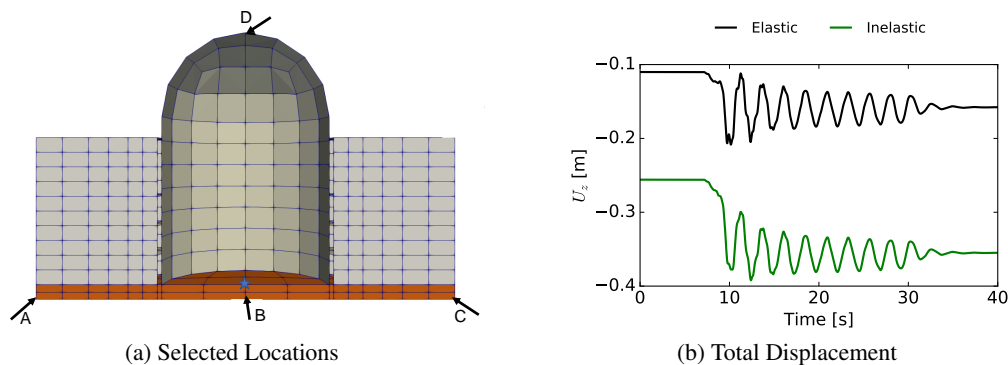


Figure 6: Locations selected to study non-linear effects and plot of total displacement at center of model *Elastic* (elastic with contact) and *Inelastic* (Elastic-Plastic with contact).

Since the site is located on the foot wall, during seismic shaking the whole structure along with soil subsides down by about 50mm in elastic and 100mm in inelastic case. Overall, if self-weight stage is also included, the soil settles by 150mm in elastic and 350mm in inelastic case as shown in Figure 6b.

It is important to predict the development of high frequency excitation during shaking because it can prove to be alarming (when close to fundamental frequency) for nuclear-equipment. These high frequencies are thus, important to be monitored, predicted during earthquakes, for design of nuclear building to ensure the safety of equipment. Figure 7 plots the acceleration and its Fourier amplitude for the location (D). It is interesting to observe, the elastic-plastic analysis kills high frequency excitations in the structure which are persistent in elastic analysis. Elastic-plastic soil shows natural damping to some high frequencies because of dissipation of energy in form of heat by hysteresis loop. This can prove to be bigly useful for safe operation of nuclear equipments even at strong seismic events. The effects of contacts coupled with elastic-plastic material leads to huge dissipation of energy reducing the high frequency modes. In Z-direction, very little significant excitation was observed.

The introduction of contact can result in opening and closing of gaps at the soil-foundation interface for stronger earthquakes. However, here for the considered seismic motion for both elastic and inelastic case with contact, no uplift was observed. Figure 8 shows the relative displacement of NPP structure for elastic and inelastic analysis at 11 seconds. In elastic case, the structure drifts a lot while the deformation in soil remains small. Whereas, in the inelastic case, the soil deforms and plastify in z-direction keeping the structure deformation small. Thus the elasto-plastic soil acts as a natural base isolators material. This demonstrates that for the considered earthquake motions, the elastic-plastic soil can prove to quite beneficial because of small deformation and excitation in structure.

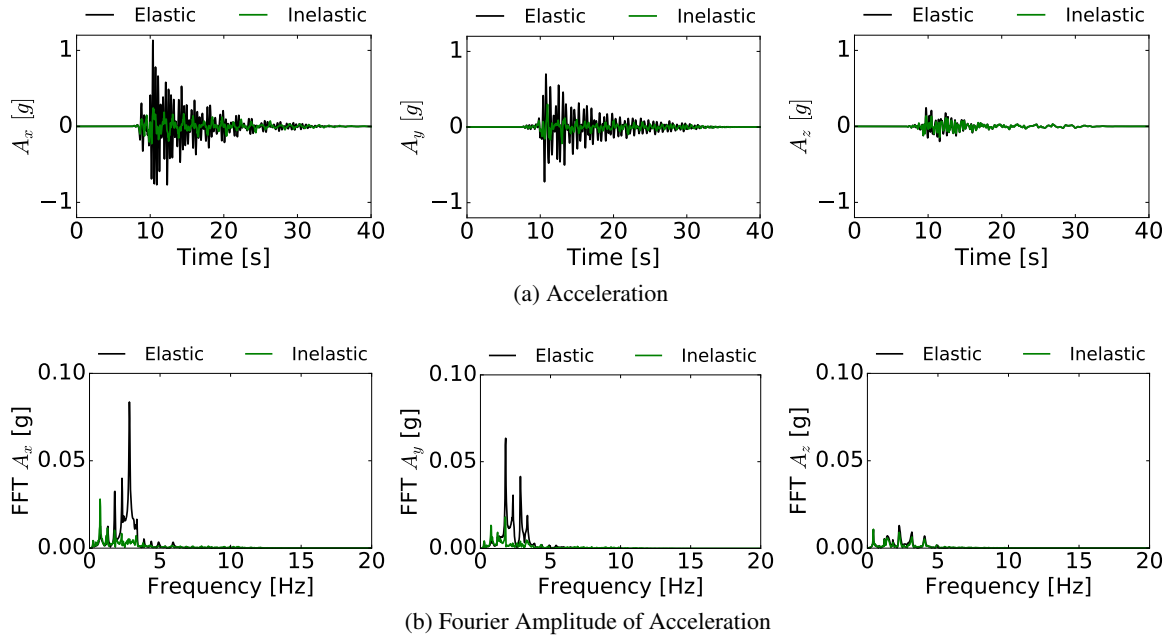


Figure 7: Seismic response at top of containment building *Elastic* (elastic without contact) and *Inelastic* (elastic-plastic with contact).

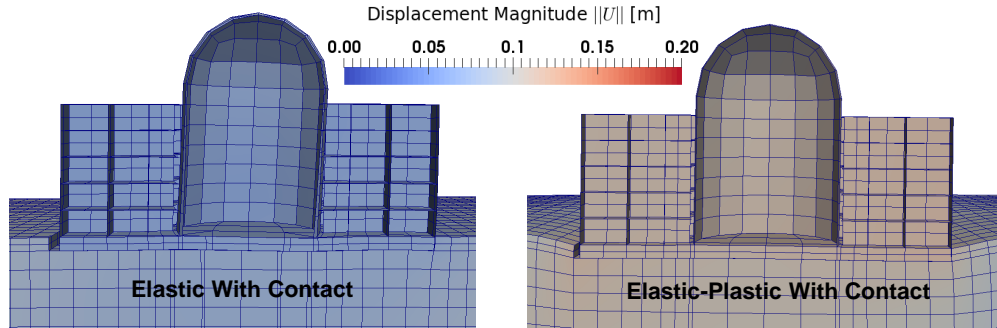


Figure 8: Deformation of the NPP structure at 11 seconds (scaled 100 times).

Figure 9 plots the inter-slip of foundation with respect to soil at location (A), (B) and (C) for elastic and elastic-plastic case with contact. It can be observed that point (A) and (B) slips both relatively towards each other describing the presence of surface waves. The center of the foundation (B) bends and slides comparatively less than the exterior ends. This also strongly shows the directivity effects of the motion coming from the $-x$ to $+x$ direction. The directivity effect is more pronounced in inelastic analysis resulting in comparatively more slip and permanent deformation. Careful observation of sliding in x -direction, shows a permanent slip of 18mm for elastic-plastic soil. Although not shown in figure, the whole NPP structure show tendency of rotation about its center of mass during the DRM stage.

ENERGY DISSIPATION

The energy dissipation in decoupled elastic plastic material under isothermal condition is given by Yang & Jeremić (2017):

$$\Phi = \sigma_{ij}\dot{\epsilon}_{ij} - \sigma_{ij}\dot{\epsilon}_{ij}^{el} - \rho\dot{\psi}_{pl} \geq 0 \quad (4)$$

where Φ is the rate of change of energy dissipation per unit volume (or dissipation density), σ_{ij} and ϵ_{ij} are the stress and strain tensors respectively, ϵ_{ij}^{el} is the elastic part of the strain tensor, ρ is the mass density

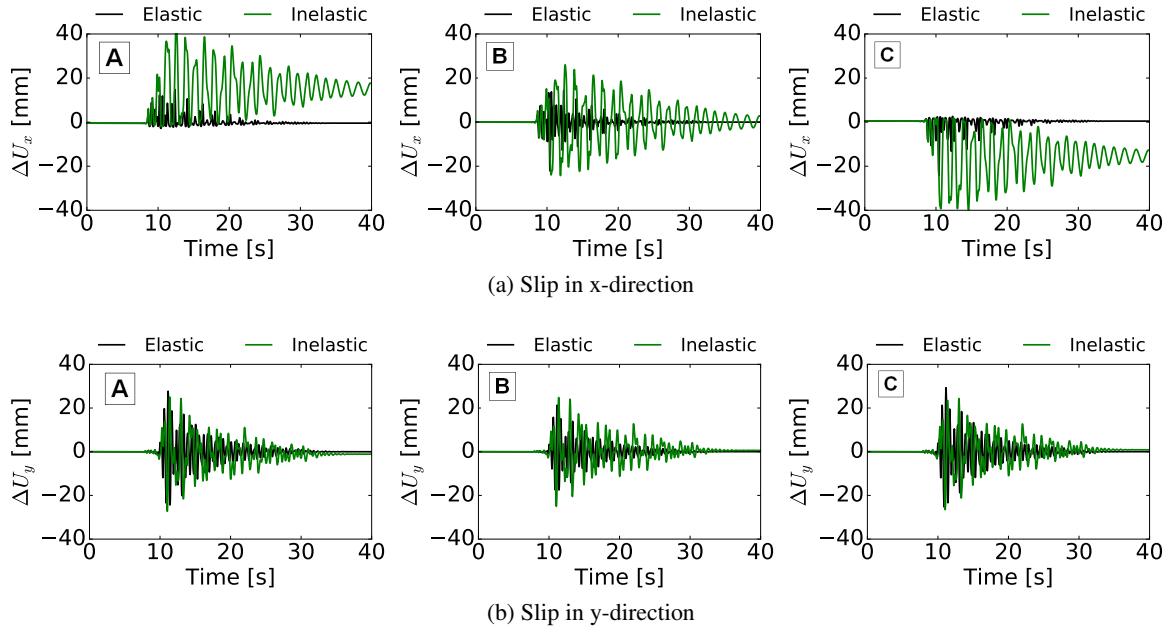


Figure 9: Slip of foundation with respect to soil beneath it in x-y slice plane for *Elastic* (elastic with contact) and *Inelastic* (Elastic-Plastic with contact).

of the material, and ψ_{pl} is the plastic free energy per unit volume (or plastic free energy density). Note that Equation 4 is derived from the first and second laws of thermodynamics, which indicate the conditions of energy balance and nonnegative rate of energy dissipation, respectively. Considering all possible forms of energy inside SSI system, the energy balance between input mechanical work W_{Input} and the combination of internal energy storage E_{Stored} and energy dissipation $E_{Dissipated}$ can be expressed as:

$$W_{Input} = E_{Stored} + E_{Dissipated} = KE + SE + PF + PD \quad (5)$$

where KE is the kinetic energy, SE is the elastic strain energy, PF is the plastic free energy, and PD is the energy dissipation due to material plasticity. Equations for each energy component can be found in Yang et al. (2017). Note that the plastic dissipation term PD includes energy dissipated in both elastic plastic solids (soil) and contact elements.

Figure 10a shows the accumulated plastic dissipation density field of the NPP model at the end of seismic event. The super-structure does not dissipate energy since it is modeled as a linear elastic material. Significant amount of seismic energy is dissipated in the contact zone between the structure and underlying soil, especially at regions around the corners and edges of the foundation. An arch-shaped elastic region is formed under the structure, where the soil moves together with the foundation and dissipates little energy. Such observation is consistent with classic bearing capacity analysis, which also indicates the formation of a relatively undeformed "active zone" beneath foundation.

As can be observed in Figure 10a, the plastic dissipation density at location (A) is the highest. From Figure 10b, it can be observed that more than 80% of the total input work is dissipated due to material plasticity or contact slipping. About 70% of the energy dissipation happens due to contact slipping, which indicates that the property and behavior of the interface between foundation and soil is crucial in SSI system. It is worth pointing out that there is about 10% of the input work transformed into plastic free energy, which falls in the typical range reported by Taylor & Quinney (1934).

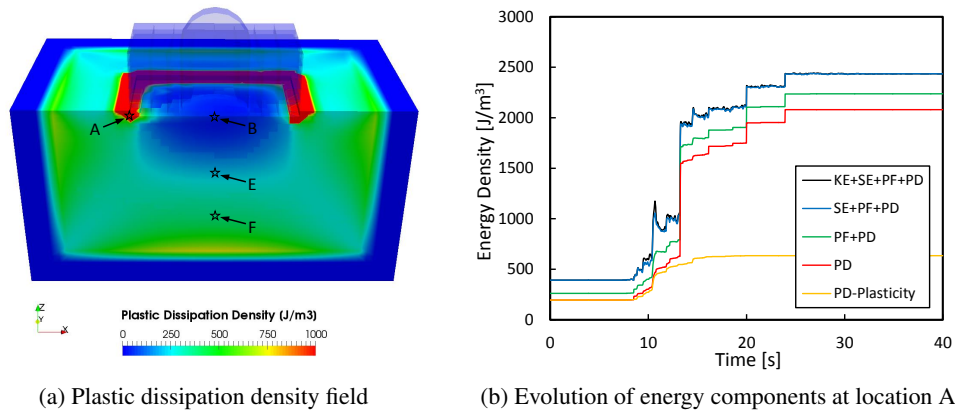


Figure 10: Energy dissipation in SMR model for inelastic (elastic-plastic soil with contact).

CONCLUSION

Presented was a high fidelity seismic simulation methodology for investigating non-linear SSI effects on NPP structures. The site being in foot-wall of the reverse thrust fault, results in permanent subsidence in vertical direction. Due to plastification, elastic-plastic soil produces comparatively more vertical settlement than linear elastic soil. It also leads to damping of some higher frequency waves. This effect of non-linear material could be beneficial to the machines which are fatal to high frequency waves. It was found that with elastic-plastic soil, there was comparatively less seismic excitation and deformation in the NPP structure for the considered seismic motion. This illustrates that the stiff soil does not necessarily help in seismic behavior of structure. This also emphasizes the fact that linear elastic modeling of soil can lead to wrong conclusions resulting in huge capital loss. With the advancement of super-computers, uncertainty in modeling can be significantly reduced by following the high-fidelity modelling techniques discussed in this paper.

The non-linear effect studied here is with respect to the specific motion (Mw 5.5 up-dip slip fault). The non-linear effect cannot be fully described using this motion itself. More similar kind of research studies using different motions and geology needs to be carried out to find out the overall non-linear and geology effects on soil-structure interaction. The author also feels that new quantities needs to be formulated to study and compare different models to categories and unify the nonlinear effects on Soil Structure Interaction (SSI) effects. Energy dissipation analysis showed that the soil close to the corners and edges of the NPP structure dissipates large amount of seismic energy. An arch-shaped elastic region was identified where design can be improved so that soil strength at these locations can contribute to the overall safety of the SSI system.

ACKNOWLEDGEMENTS

Funding from and collaboration with US-DOE and CNSC is much appreciated.

REFERENCES

- Bielak, J. (1978), 'Dynamic response of non-linear building-foundation systems', *Earthquake Engineering & Structural Dynamics* **6**(1), 17–30.
- Bielak, J., Loukakis, K., Hisada, Y. & Yoshimura, C. (2003), 'Domain reduction method for three-dimensional earthquake modeling in localized regions. part I: Theory', *Bulletin of the Seismological Society of America* **93**(2), 817–824.

- Chopra, A. K. & Gutierrez, J. A. (1974), 'Earthquake response analysis of multistorey buildings including foundation interaction', *Earthquake Engineering & Structural Dynamics* **3**(1), 65–77.
- Dafalias, Y. F. & Manzari, M. T. (2004), 'Simple plasticity sand model accounting for fabric change effects', *ASCE Journal of Engineering Mechanics* **130**(6), 622–634.
- Dafalias, Y., Schick, D., Tsakmakis, C., Hutter, K. & Baaser, H. (2002), A simple model for describing yield surface evolution, in 'Lecture note in applied and computational mechanics', Springer, pp. 169–201.
- Dickenson, S. E. (1994), Dynamic response of soft and deep cohesive soils during the Loma Prieta earthquake of October 17, 1989, PhD thesis, University of California, Berkeley.
- Elgamal, A., Yan, L., Yang, Z. & Conte, J. P. (2008), 'Three-dimensional seismic response of humboldt bay bridge-foundation-ground system', *ASCE Journal of Structural Engineering* **134**(7), 1165–1176.
- Jeremić, B., Jie, G., Cheng, Z., Tafazzoli, N., Tasiopoulou, P., Abell, F. P. J. A., Watanabe, K., Feng, Y., Sinha, S. K., Behbehani, F., Yang, H. & Wang, H. (2017), *The Real ESSI Simulator System*, University of California, Davis and Lawrence Berkeley National Laboratory. <http://real-essi.info/>.
- Jeremić, B., Jie, G., Preisig, M. & Tafazzoli, N. (2009), 'Time domain simulation of soil–foundation–structure interaction in non–uniform soils.', *Earthquake Engineering and Structural Dynamics* **38**(5), 699–718.
- Jeremić, B., Kunnath, S. & Xiong, F. (2004), 'Influence of soil–foundation–structure interaction on seismic response of the i-880 viaduct', *Engineering Structures* **26**(3), 391–402.
- Lou, M., Wang, H., Chen, X. & Zhai, Y. (2011), 'Structure–soil–structure interaction: literature review', *Soil Dynamics and Earthquake Engineering* **31**(12), 1724–1731.
- Petersson, N. A. & Sjögreen, B. (2017), 'High order accurate finite difference modeling of seismo-acoustic wave propagation in a moving atmosphere and a heterogeneous earth model coupled across a realistic topography', *Journal of Scientific Computing* pp. 1–34.
- Rodgers, A. (2017), Private communications, SW4 – Real ESSI connection.
- Rosakis, P., Rosakis, A., Ravichandran, G. & Hodowany, J. (2000), 'A thermodynamic internal variable model for the partition of plastic work into heat and stored energy in metals', *Journal of the Mechanics and Physics of Solids* **48**(3), 581–607.
- Sinha, S. K. & Jeremić, B. (2017), 3D contact modeling for soil structure interaction, Technical report, University of California, Davis.
- Taylor, G. I. & Quinney, H. (1934), 'The latent energy remaining in a metal after cold working', *Proceedings of the Royal Society of London. Series A, Containing Papers of a Mathematical and Physical Character* **143**(849), 307–326.
- Tyapin, A. (2007), 'The frequency–dependent elements in the code SASSI: A bridge between civil engineers and the soil–structure interaction specialists', *Nuclear Engineering and Design* **237**, 1300–1306.
- Wair, B. R., de Jong, J. T. & Shantz, T. (2012), Guidelines for estimation of shear wave velocity profiles, Technical Report 8, PEER. 95 pages.
- Watanabe, K., Pisanò, F. & Jeremić, B. (2016), 'A numerical investigation on discretization effects in seismic wave propagation analyses', *Engineering with Computers* pp. 1–27.
- Yang, H. & Jeremić, B. (2017), 'Energy dissipation analysis of elastic-plastic structural elements [manuscript in preparation]'.
- Yang, H., Sinha, S. K., Feng, Y., McCallen, D. B. & Jeremić, B. (2017), 'Energy dissipation analysis of elastic-plastic materials [manuscript submitted for publication]'.
- Yang, Z., Elgamal, A. & Parra, E. (2003), 'Computational model for cyclic mobility and associated shear deformation', *Journal of Geotechnical and Geoenvironmental Engineering* **129**(12), 1119–1127.